



Western Michigan University
ScholarWorks at WMU

Honors Theses

Lee Honors College

4-3-2024

A Petrological Characterization of the Iutzi Member of Lucas Formation, Michigan Basin

Moira Burns
Western Michigan University

Follow this and additional works at: https://scholarworks.wmich.edu/honors_theses



Part of the Geology Commons

Recommended Citation

Burns, Moira, "A Petrological Characterization of the Iutzi Member of Lucas Formation, Michigan Basin" (2024). *Honors Theses*. 3790.

https://scholarworks.wmich.edu/honors_theses/3790

This Honors Thesis-Open Access is brought to you for free and open access by the Lee Honors College at ScholarWorks at WMU. It has been accepted for inclusion in Honors Theses by an authorized administrator of ScholarWorks at WMU. For more information, please contact wmu-scholarworks@wmich.edu.



A Petrological Characterization of the Iutzi Member of Lucas Formation, Michigan Basin

Moira A. Burns

Abstract/Summary:

It is thought that most Phanerozoic dolomites form via the replacement of precursor calcium carbonate [CaCO_3] with dolomite [$\text{CaMg}(\text{CO}_3)_2$] through a dissolution-precipitation reaction with a Mg-bearing fluid. Although this may be widely accepted, the timing, conditions, settings, and mechanisms associated with the dolomitization process are still strongly debated, resulting in the proposal of various dolomitization models. The association between evaporite minerals and dolomite in the rock record is common and has led many to propose a model genetically associating evaporative fluids and dolomitization. The evaporative model posits as marine fluids evaporate and become more concentrated, gypsum [$\text{CaSO}_4 \cdot 2\text{H}_2\text{O}$] precipitates, increasing the Mg:Ca ratio of the fluids. Dolomitization is favored as these dense Mg-rich brines infiltrate and flow downward through the underlying carbonates. Although this model is theoretically robust, it has been criticized, as evidence of downward refluxing brines is scarce.

In the current study, newly acquired petrographical (thin section, scanning electron microscopy), mineralogical (powder x-ray diffraction), bulk elemental (x-ray fluorescence), micro-scale elemental (SEM-energy dispersive spectroscopy), and conventional stable isotope data are used to evaluate test the evaporative reflux model in the evaporite associated dolomites of the informal “Massive Anhydrite” unit in the Iutzi Member of the Lucas Formation in the Michigan Basin. The studied interval (2117.5-2118.5 ft) in the Brown Snowplow #1-5, Alpena Co., Michigan is characterized by nodular-anhydrite crystals (10-20 micrometers) and small dolomite rhombohedra (<10 micrometers), which occur between anhydrite nodules and as

inclusions within anhydrite nodules. Microcrystalline dolomites are isotopically light ($\delta^{18}\text{O} = -5.88 \text{ ‰ VPDB}$) and formed prior to the precipitation of the gypsum/anhydrite characterized in the “Massive Anhydrite” unit. Collectively, these observations are inconsistent with the evaporative reflux model for dolomitization.

Introduction:

Dolomite [$\text{CaMg}(\text{CO}_3)_2$] is an abundant sedimentary mineral in the ancient rock record, but rare in modern settings (see reviews by Hardie, 1987; Land, 1985; Machel, 2004; Gregg et al., 2015; Kaczmarek et al., 2017). In order to explain the vast dolomite deposits in the rock record, multiple dolomitization models have been proposed (Machel, 2004). While various models disagree on the conditions, timing, and setting of dolomitization, it is widely accepted that most Phanerozoic dolomites are formed via a dissolution-precipitation process whereby calcite or aragonite [CaCO_3] in a precursor sediment or rock is replaced by dolomite during a reaction that takes place in a magnesium [Mg^{2+}] bearing fluid (Land, 1985). This process is easy to replicate in the laboratory at elevated temperatures (e.g., Kaczmarek and Sibley, 2007, 2011, 2014; Kaczmarek and Thornton, 2017) but attempts to dolomitize CaCO_3 in the laboratory at temperatures below 100°C , have been largely unsuccessful (Gregg et al., 2015; Kaczmarek et al., 2017). Moreover, because modern dolomites are rare, natural analogs are few and far between (Hardie, 1987; Machel 2004). The failure to make dolomite in the laboratory at Earth surface conditions combined with the lack of modern examples leaves many questions about the environment, timing, and conditions of ancient dolomite formation. Such interpretations of natural dolomite are based on a wide variety of petrological data, which lead to an equally wide variety of models that attempt to explain the timing, temperature, and fluid compositions involved with dolomitization (Machel, 2004; Manche and Kaczmarek, 2021).

One of the most commonly cited dolomitization models claims that dolomite formation in sedimentary environments is driven by highly concentrated fluids formed via evaporation of marine waters that have become restricted. This model is based on important empirical observations as well as a suite of theoretical considerations. Commonly cited are (i) the abundance of dolomites in shallow water marine compared to deeper water deposits, and (ii) the co-occurrence of evaporite minerals and dolomite in the rock record (Land, 1985). Adams and Rhodes (1960) were the first to propose that dolomitization by seepage refluxion of evaporative fluids in a restricted lagoon explains the high percentage of bedded dolomites associated with evaporites. The idea for this model was based on mineralogical evidence of evaporite pore filling cements observed within Permian dolomites and also by observing an increase in the presence of evaporites up section (Adams and Rhodes, 1960). The theoretical basis for the evaporative fluid model is based on elevated temperatures and chemical conditions that promote dolomite formation. First, the model posits that when the fluids become concentrated enough, gypsum [$\text{CaSO}_4 \cdot 2\text{H}_2\text{O}$] precipitates, thus causing the increase of the Mg:Ca ratio of fluids to create a chemical condition that strongly promotes dolomite formation (Adams and Rhodes, 1960). The elevated temperatures associated with these restricted settings also favors dolomite formation (Adams and Rhodes, 1960).

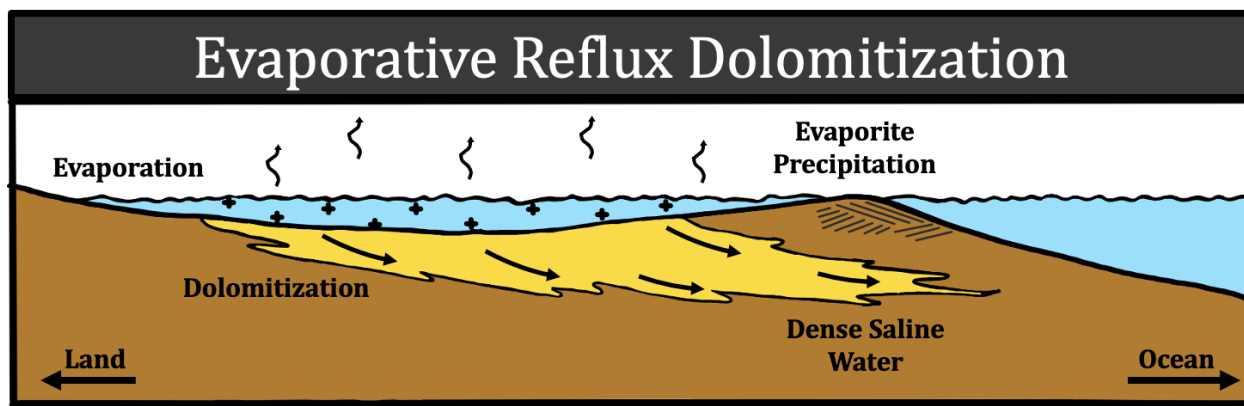


Figure 1. (Preceding page) Conceptual model of reflux dolomitization. As marine fluids evaporate and become more concentrated, gypsum [$\text{CaSO}_4 \cdot 2\text{H}_2\text{O}$] precipitates, increasing the Mg:Ca ratio of fluids. Dolomitization is favored as dense brines hydrologically flow downward (modified after James and Jones).

The evaporative reflux model also posits a hydrological mechanism for these warm, dense fluids to migrate downward, thus delivering Mg and removing Ca. In summary, the model suggests that dolomitization is promoted through the downward hydrological flow of the elevated Mg/Ca dense brines through underlying carbonate sediments (Machel, 2004; Manche and Kaczmarek, 2019).

Despite what appears to be a strong theoretical basis, convincing empirical evidence of dolomitization by highly evaporative fluids is sparse, as pointed out by a number of recent papers (e.g., Ryan et al., 2020; Laya et al., 2021). And yet, the evaporative reflux model is one of the most commonly cited models in the literature (S. Kaczmarek, personal communication). In fact, Adams and Rhodes (1960) has been cited nearly one-thousand times at the time of writing.

The current study attempts to add to this conversation through a detailed petrological characterization of the co-occurring evaporites and dolomites in the Iutzi Member of the Devonian Lucas Formation in the Michigan Basin. Preliminary work on these rocks was conducted as part of a class project for GEOS 5100: Advanced Earth Materials. These preliminary results were presented at the northcentral Geological Society of America conference

by Burns et al. (2023) In summary, key observations include dolomite crystals inclusions within anhydrite [CaSO₄] nodules, which suggests that the dolomite formed prior to the anhydrite. The absolute timing of the minerals is unknown, leaving the genetic relationship between them also in question. The current study expands on the work of Burns et al. (2023) by adding additional petrographic, mineralogical, and geochemical data to better constrain the timing, conditions, and fluids associated with dolomitization of the Iutzi Member of the Lucas Formation. More specifically, this research aims to present another test the reflux dolomitization hypothesis using the Iutzi Member of the Lucas Formation as a case study.

Geological Background of the Lucas Formation

During the Devonian Period, the Michigan Basin was subjected to several marine transgressions and regressions, which resulted in deposition of repetitive sedimentary rock layers composed of dolomite, anhydrite, salt, limestone, and sandstone. Through the use of well logs, drill cores, drillers' records and literature, the uppermost section of rock known as the Lucas Formation of the Detroit River Group has been interpreted to have formed in restricted marine environments. (Gardner, 1974; Apak, 1985; Park, 1987). The Lucas Formation is historically divided into three stratigraphic members (Figure 2). From oldest to youngest, the members of the Lucas Formation include the Richfield, the Iutzi, and the Horner members (Gardner, 1974 and Park, 1987).

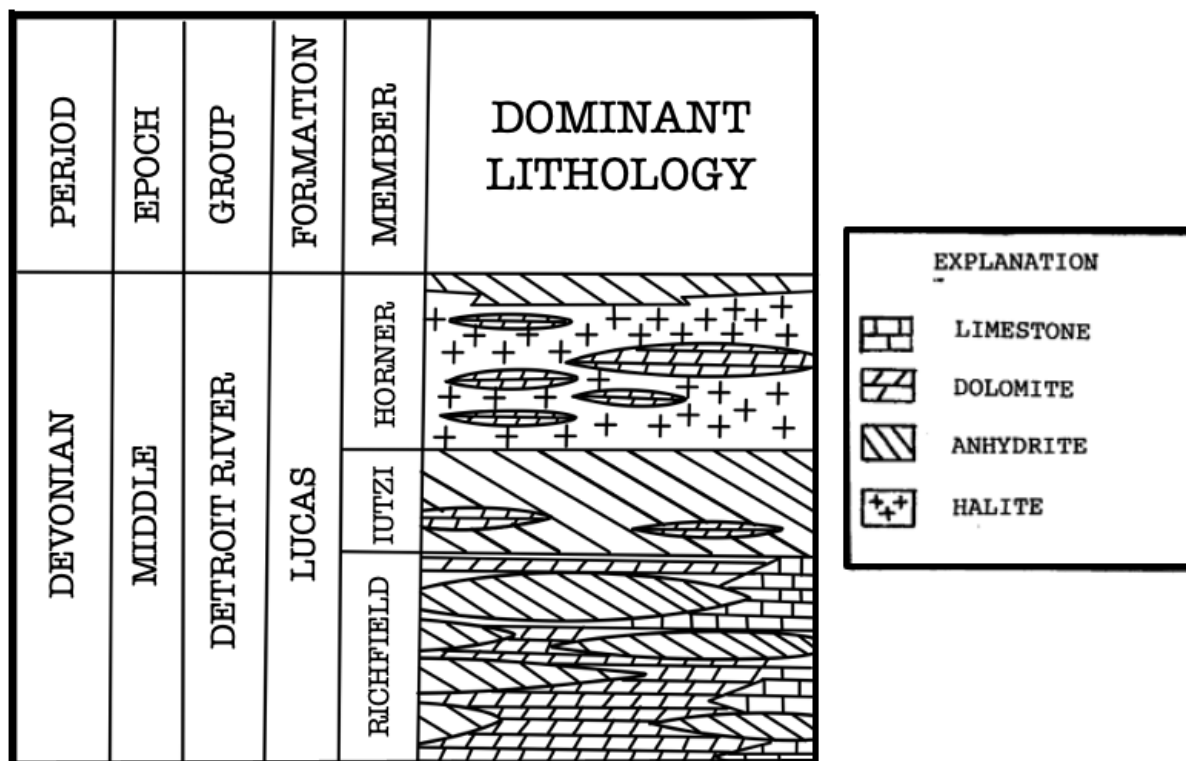


Figure 2. Stratigraphic column and nomenclature for the Lucas Formation (Modified from Gardner, 1974 and Park 1987).

Consisting primarily of beds of dolomite and anhydrite, as well as some limestone lenses, the Richfield Member is an important oil-bearing horizon in the Michigan Basin (Lilienthal, 1978; Park, 1987). Above the Richfield Member, lies the Iutzi Member, which is composed of thick deposits of gypsum. The Iutzi marks an extensive evaporite depositional period within the Michigan Basin (Park, 1987). Within the Iutzi Member lies an informal stratigraphic unit known as the “Massive Anhydrite.” Near the center of the Michigan Basin, the “Massive Anhydrite” is roughly 100 feet thick. Toward the edges of the basin the unit undergoes a lateral facies change to dolomite. The uppermost portion of the Iutzi is characterized by interbedded limestones and dolomites along with thick beds of anhydrite (Gardner, 1974; Park, 1987). Above the Iutzi Member lies the Horner Member, which is composed of thick deposits of halite and gypsum that thicken toward the center. The Horner Member was presumably deposited during a period of

extensive evaporation within the Michigan Basin (Park, 1987). Within the lower carbonates of the Horner is an informal unit referred to as the “sour zone”, which got its name from the potent sulfurous odor of the core samples and also from the sulfur-rich crude oil that is produced from this zone.

Iutzi Member

The focus of the current study is the “Massive Anhydrite,” the informal unit that is a part of the Iutzi Member. The lateral persistence and thickness of this unit has been cited as strong evidence for the basin to have experienced evaporite mineral deposition (Park 1987). For thick packages of anhydrite to form, the hydrologic conditions, salinity, and subsidence must remain consistent for extended periods of time. (Gardner 1974). Evidence for the “Massive Anhydrite” to be of subaqueous depositional origin is based on the scarcity of carbonate mud, the thickness across the center of the basin as well as the change to carbonates on the outer edges of the Michigan Basin (Park 1987).

Methods:

This study focuses on a 1.5 ft section of core (2118.5 – 2117.5 ft) in the Brown Snowplow #1-5 core in Alpena County, Michigan. All analytical measurements were conducted on a single rock sample that was collected from a depth of approximately 2118.0 ft. The sample comes from the informal stratigraphic unit known as the “Massive Anhydrite” within the Iutzi Member of the Lucas Formation. A full petrological characterization of the sample was performed following standard analytical methods and petrological workflow developed in the Carbonate Petrology and Characterization Laboratory. Details of this workflow and methods are discussed in Ryan et

al. (2020). Textural, mineralogical, and geochemical data were collected using a suite of analytical instruments, which are summarized in Table 1.

Table 1. Summary of Analytical Methods

Method	Data Collected	Analytical Parameters	References
pXRD (Powder x-ray diffraction)	Bulk mineralogy Dolomite stoichiometry	Bruker 2D Phaser X-Y range 2 θ : 5°-105° Step Size: 0.020° Time/Step: 1sec/step Wavelength: 1.5406 Å (Cu K α)	Kaczmarek et al. (2017) Gregg et al. (2015)
XRF (X-ray fluorescence)	Bulk elemental concentrations for elements heavier than sodium [Na ¹⁺]	Bruker tracer IV-SD Each measurement was done in tandem. Low energy mode: 15 kV and 35 μ A for 60 seconds High energy mode: 40 kV and 40 μ A for 90 seconds.	Al-Musawi & Kaczmarek (2020)
SEM-SE (scanning electron microscopy-secondary electrons)	Topographic information of sample surface, high resolution petrographic information	JEOL JSM IT100 InTouchScope Sample coated in carbon to create an electrically conductive surface. Accelerating voltage of 20 kV Working distance of 11 mm, Probe current 23-60 HV. Exact parameters set to maximize image quality and resolution.	Ryan et al. (2020)
SEM-BSE (scanning electron microscopy-back scatter)	Compositional information sample, Grayscale images track materials with different atomic masses	Coated in carbon to create a conductive layer. Used an accelerating voltage of 20 kV, working distance of 11 mm, and a probe current ranging from 23-60 HV using a JOEL JSM IT100 InTouchScope. Imaged at 350x magnification.	Ryan et al. (2020)
Thin Section Petrography	Petrographic information, Imaging Rock texture, mineral assemblage, etc.	Standard thin sections impregnated with blue epoxy to highlight pores, stained with Alizarin-Red-S (ARS) to differentiate between dolomite and calcite. Slides were polished to 30 micrometer thickness.	Ryan et al. (2020)
SEM-EDS (scanning electron microscopy-energy dispersive spectroscopy)	In situ point analysis, Elemental maps, Elemental composition	JEOL JSM IT100 InTouchScope Instrument parameters set to maximize data quality.	Ryan et al. (2020)
Conventional Isotope Analysis	Oxygen isotope reported in permil $\delta^{18}\text{O}$ notation relative to VPDB	Sample reacted in borosilicate reaction vessel with 4 drops of phosphoric acid at 77 ° C for 12 min in a Finnigan MAT Kiel IV preparation device coupled to the inlet of a Finnigan MAT 253 triple collector isotope ratio mass spectrometer.	Ryan et al. (2020)

Results:

The studied interval (2117.5-2118.5 ft) of the Brown Snowplow 1-5 Core from Alpena County, MI is characterized by large blue nodules that vary in size from 1 to 8 cm in diameter. The largest nodules occur at a depth of 2118.0 ft and decrease in size above and below that depth. Between the blue nodules is a brown fine-grained matrix that when scratched, fizzes when exposed to dilute (10%) hydrochloric acid (HCl). The texture of the core resembles a common sedimentary texture known as chicken wire anhydrite (Figure 3).



Figure 3. Photograph of slabbed Brown Snowplow 1-5 Core from Alpena County, MI. Depth ranging from 2117.5-2118.5ft below the surface. Located within an informal unit of the Iutzi Member of the Lucas Formation known as the “Massive Anhydrite”. The core exhibits large blue nodules that vary in size and are separated by a fine brown matrix.

Thin Section Petrography:

Under plane polarized light (PPL) (Figures 4A and 5A) and cross-polarized light (XPL) , the blue nodules show medium relief (Figures 4B and 5B) and are fibrous and angular. Crystals are anisotropic and show a medium birefringence consistent with properties of anhydrite [CaSO₄]. Because of its fine crystalline texture, the brown matrix material could not be characterized mineralogically based on thin section observations alone.

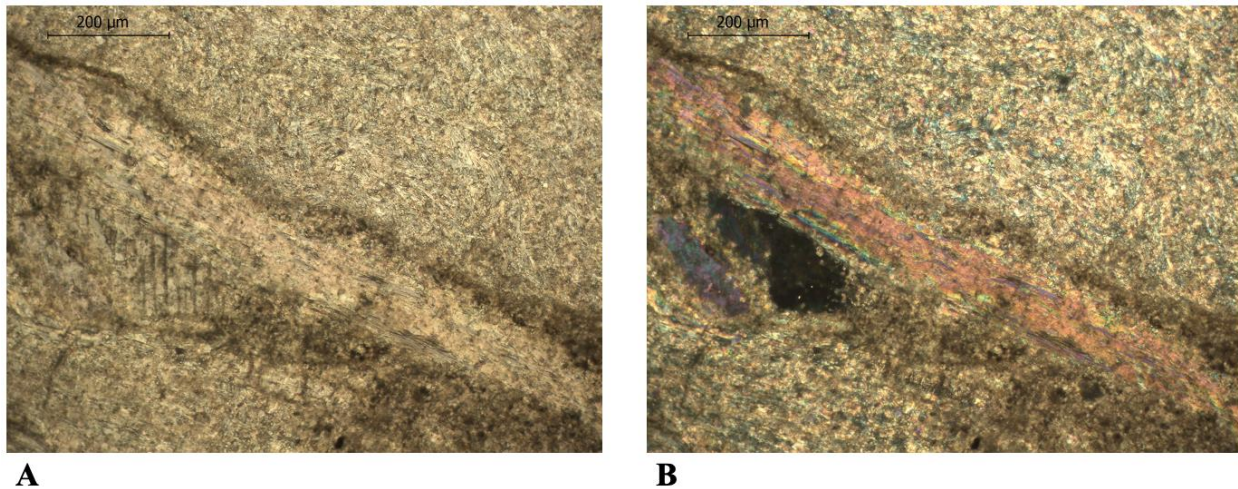


Figure 4. Micrographs of thin section samples in plane polarized (PPL) and cross polarized light (XPL) of blue (anhydrite) nodules and brown fine crystalline (dolomite) matrix. In PPL, blue anhydrite nodules appear fibrous, angular, and light tan in color. In XPL, the fibrous anhydrite nodules are angular, show medium relief, have a higher refractive index, and are anisotropic. Individual crystals in the brown matrix cannot be resolved. **(A)** Micrograph at 100x of thin section sample in plane polarized light (PPL). **(B)** Micrograph at 100x of thin section sample in plane polarized light (XPL).

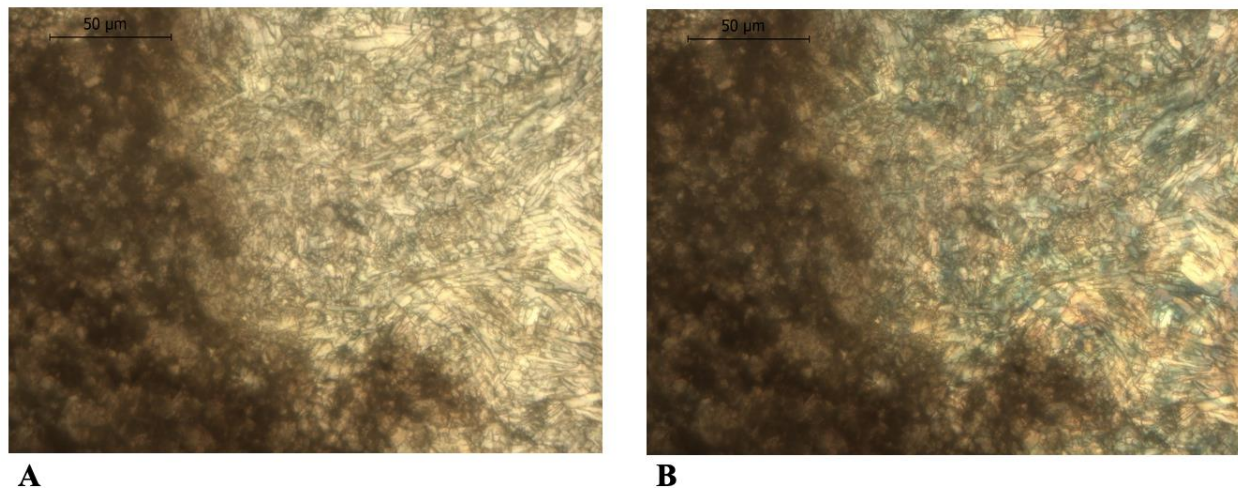


Figure 5. (Previous page) Micrographs of thin section samples in plane polarized (PPL) and cross polarized light (XPL) of blue (anhydrite) nodules and brown fine crystalline (dolomite) matrix. In PPL, blue anhydrite nodules appear fibrous, angular, and light tan in color. In XPL, the fibrous anhydrite nodules are angular, show medium relief, have a higher refractive index, and are anisotropic. Individual crystals in the brown matrix cannot be resolved. **(A)** Micrograph at 400x of thin section sample in plane polarized light (PPL). **(B)** Micrograph at 400x of thin section sample in plane polarized light (XPL).

Powder X-Ray Diffraction (pXRD):

Two sub-samples from the core were analyzed. One sub-sample targeted the blue nodules. The other targeted the brown matrix. The blue nodule sub-sample is characterized by anhydrite and the brown matrix sub-sample is characterized by anhydrite and a very minor amount of dolomite.

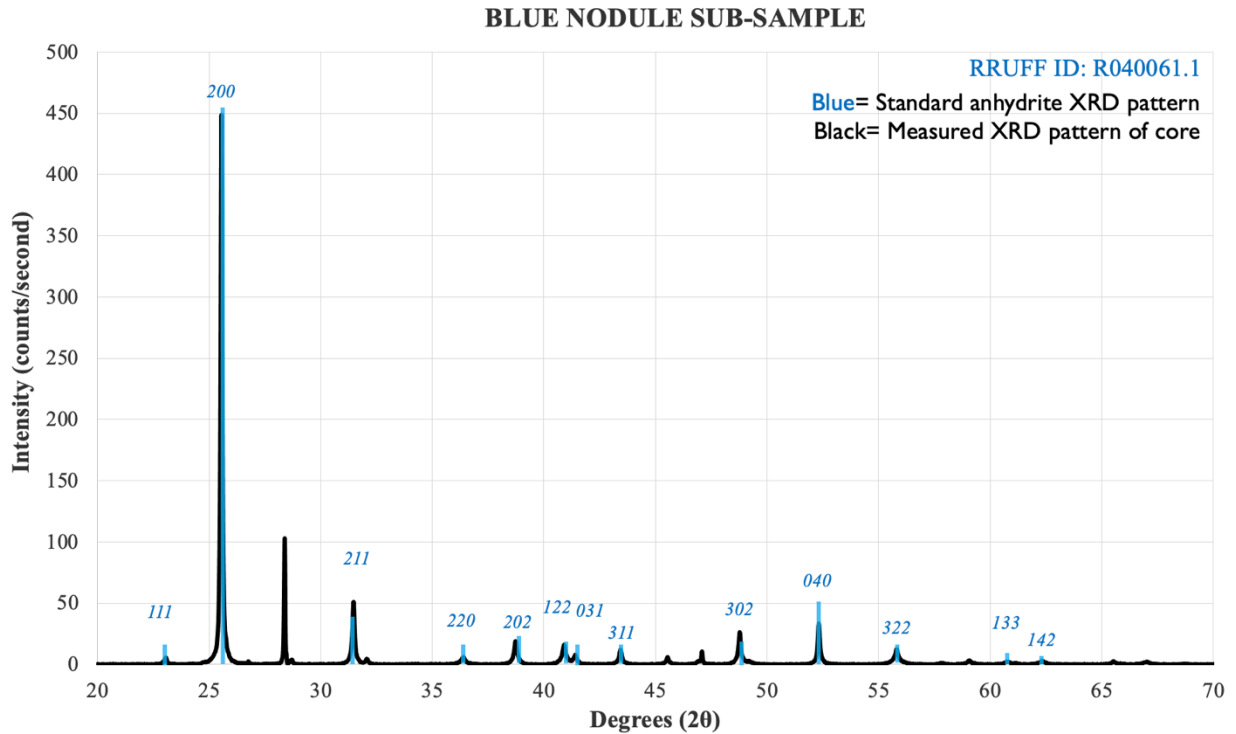


Figure 6. Powder XRD patterns comparing anhydrite from lab sample (in black) to an anhydrite standard (in blue). Anhydrite peaks are labelled with their corresponding Bravais-Miller indices (Downs et al., 1993).

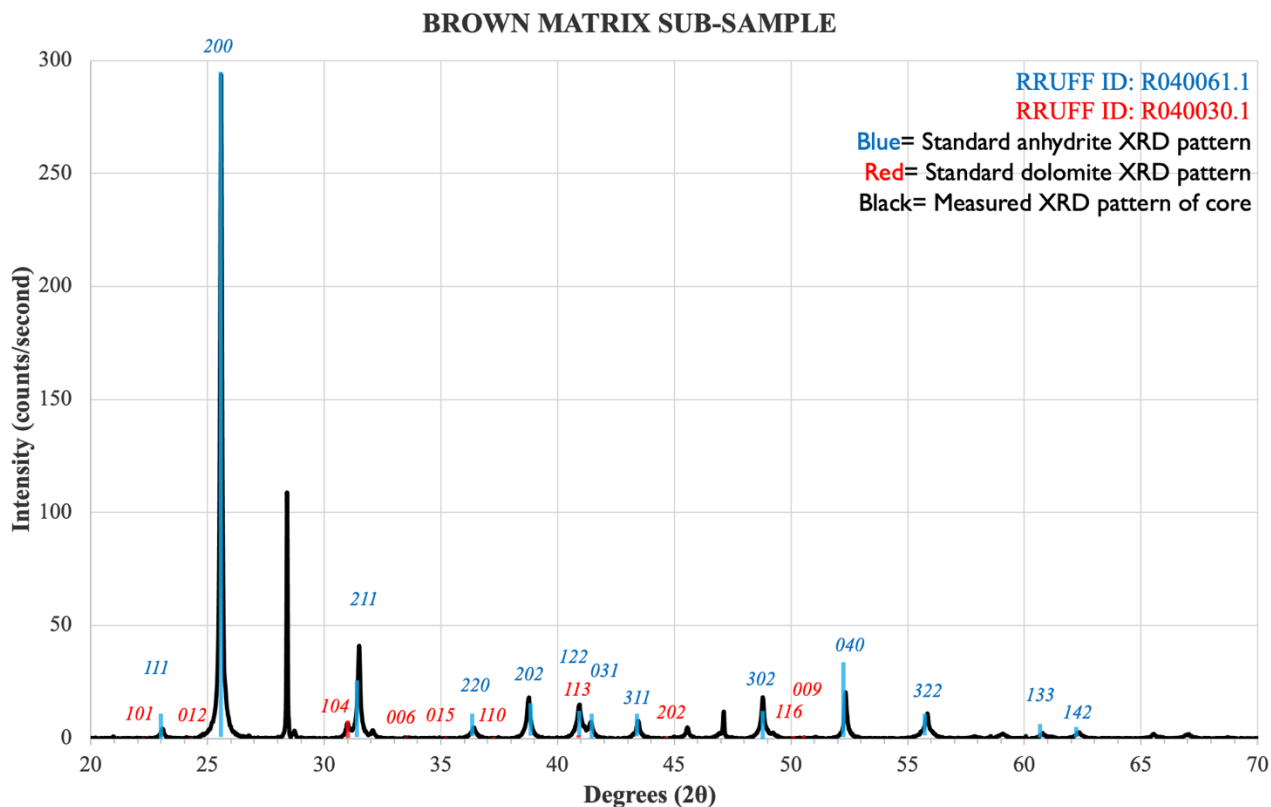


Figure 7. Powder XRD pattern for the brown matrix sample (in black). The anhydrite standard (in blue) and dolomite standard (in red) are also shown. Dolomite and anhydrite peaks are labelled with their corresponding Bravais-Miller indices (Downs et al., 1993).

The XRD pattern from the blue nodules shows peak positions and relative intensities that correspond with the published standard for anhydrite (Figure 6). XRD peaks are labeled with their corresponding Miller indices, which come from the American Mineralogist Crystal Structure Database (Downs et al., 1993). Dolomite peaks are not present in the blue nodule sample. The XRD pattern for the brown matrix sub-sample shows peak positions and intensities that also match well with the anhydrite standard. A small dolomite 104 peak is also visible at 30.99 degrees two-theta (Figure 7).

Based on the position of the $d_{(104)}$ dolomite reflection, the stoichiometry (mole% MgCO_3) was determined using the empirical equation from Lumsden and Chimahusky (1980). In carbonate rocks, the interplanar d-spacing can be calculated using a function of the 2θ peak position. The

smaller the 2θ diffraction angle, the larger the interplanar d-spacing, which indicates Ca enrichment in dolomite as the larger Ca ions occupy the lattice positions where smaller Mg ions typically reside (Kaczmarek and Sibley, 2011). The position of the $d_{(104)}$ peak in the standard occurs at $30.99^\circ 2\theta$ and has a d-spacing of 2.886 Angstroms (Kaczmarek et al., 2017). Although small, the measured position of the $d_{(104)}$ peak in Figure 7 also occurs at $30.99^\circ 2\theta$, the d-spacing is also 2.886 Angstroms. This d-spacing is then used in the Equation 1 from Lumsden and Chimahusky (1980) to calculate a dolomite stoichiometry of 50% mol% MgCO_3 .

$$\text{dolomite mol\% MgCO}_3 = 1 - [333.3 * d[104] - 911.99] \quad (\text{Equation 1})$$

A dolomite cation ordering value could not be determined due to the low intensities of the dolomite ordering peaks.

XRF:

XRF analysis showed that $[\text{Ca}^{2+}]$, $[\text{S}^{2-}]$, and $[\text{Mg}^{2+}]$ exhibit high abundances. This is not surprising given the main mineral compositions of anhydrite $[\text{CaSO}_4]$ and dolomite $[\text{CaMg}(\text{CO}_3)_2]$. Lower abundances of aluminum $[\text{Al}^{3+}]$, chromium $[\text{Cr}]$, iron $[\text{Fe}]$, nickel $[\text{Ni}^{2+}]$, and titanium $[\text{Ti}^{3+}]$ are also observed.

Table 2. PXRF data displaying energy element abundances expressed as photon counts for both the sampled anhydrite $[\text{CaSO}_4]$ nodules and dolomite $[\text{CaMg}(\text{CO}_3)_2]$ matrix.

Element Abundances Expressed as Photon Counts			
	Blue Nodules	Brown Matrix	High or Low Energy
Ca	1058338	1088186	Low
Mg	2703	3167	Low
S	1036260	953832	Low
Fe	1786	2210	Low
Al	829	757	Low
Ti	2012	1916	Low
Sr	23795	22993	High

SEM-SE & SEM-EDS:

SEM-SE micrographs show rhombic crystals within a blocky saccharoidal ground mass (Figs. 8, 9, and 10). As shown in Figures 9 and 10, elemental compositions of the rhombic minerals (i.e., high [Mg], [Ca]) and the ground mass (i.e. high [Ca], [S]) are consistent with the presence of dolomite [$\text{CaMg}(\text{CO}_3)_2$] and anhydrite [CaSO_4], respectively. Oxygen [O] and carbon [C] in the EDS data are consistent with the presence of anhydrite and dolomite but are unable to distinguish between these two minerals.

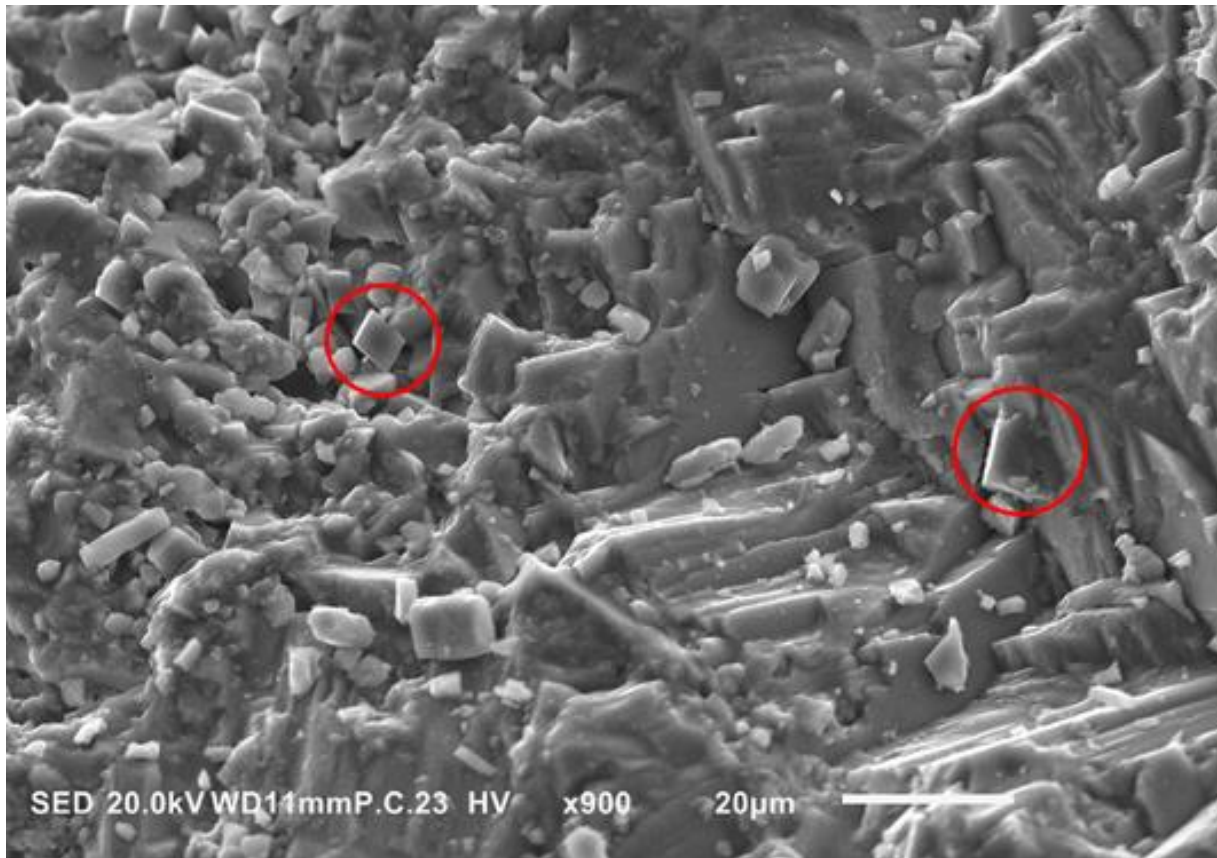


Figure 8. SEM-SE photomicrograph of the nodular-anhydrite from the Lucas Formation in the Michigan Basin at 900x shows dolomite rhomboid inclusions (circled in red) within the anhydrite nodules. Crystal size of the dolomite rhomboids are less than 10 micrometers.

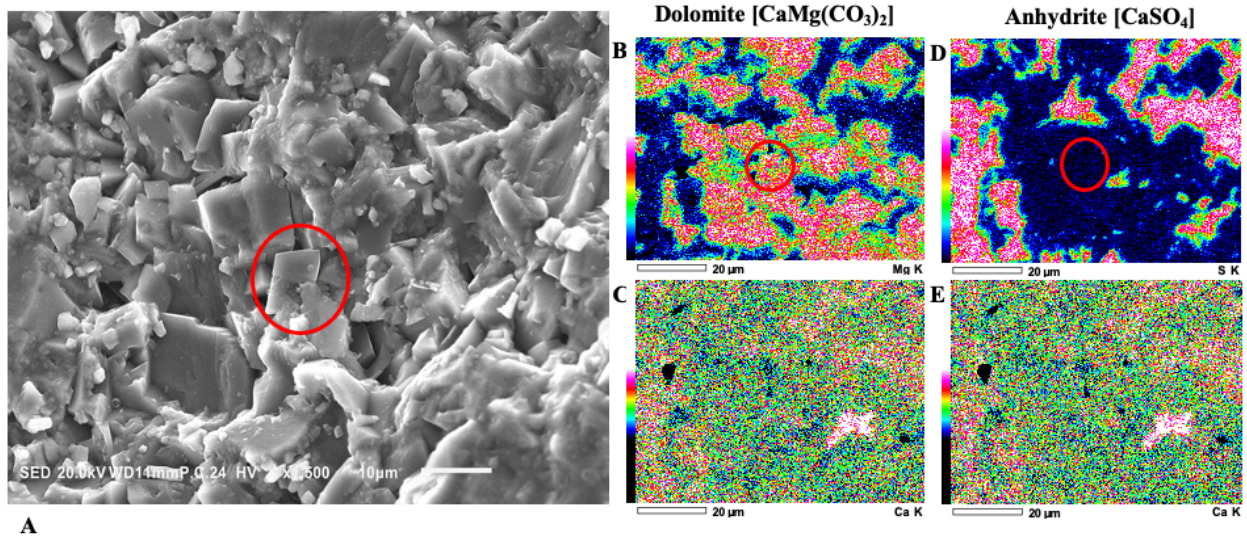


Figure 9. SEM-SE and SEM-EDS photomicrographs of dolomite inclusions within nodular-anhydrite. (A) SEM-SE photomicrograph at 1,500x of rhomboid inclusions (circled in red) within anhydrite nodules supported by (B) and (C) SEM-EDS elemental maps of dolomite $[\text{CaMg}(\text{CO}_3)_2]$ and its corresponding elements $[\text{Mg}^{2+}]$ and $[\text{Ca}^{2+}]$. (D) and (E) SEM-EDS elemental maps of anhydrite $[\text{CaSO}_4]$ and its corresponding elements $[\text{S}^{2-}]$ and $[\text{Ca}^{2+}]$. Elemental data is depicted as higher readings of a specific element in white/pink and lower readings in darker green/blue. Crystal sizes of the anhydrite range from 10-20 μm and the small dolomite rhomboids are less than 10 μm .

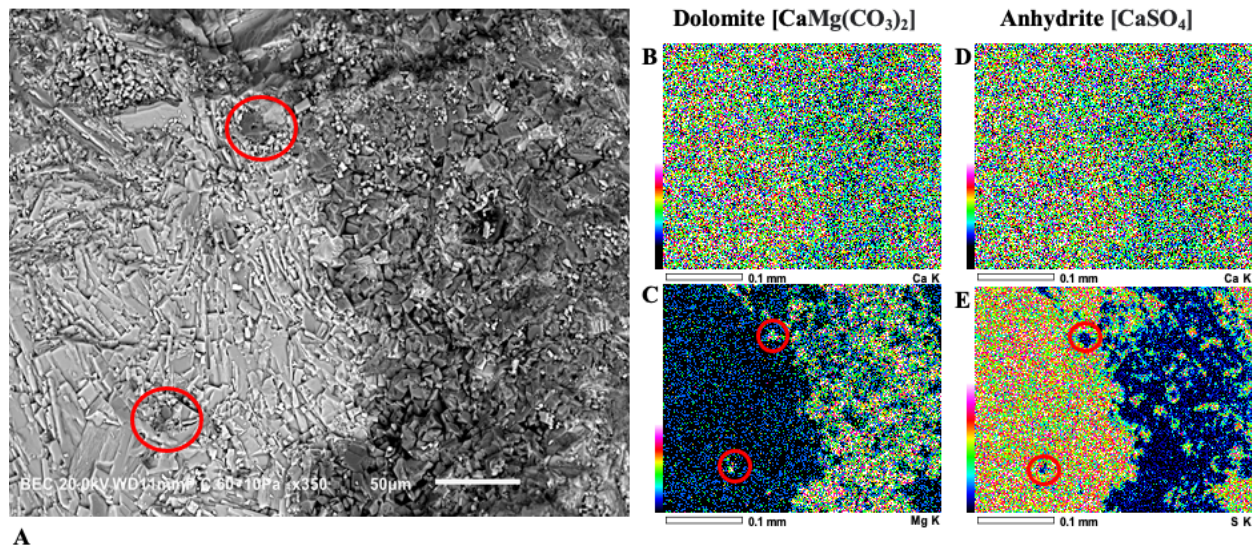


Figure 10. SEM-SE and SEM-EDS photomicrographs of nodular-anhydrite. **(A)** SEM-SE photomicrograph at 350x of rhomboid inclusions (circled in red) within anhydrite nodules supported by **(B)** and **(C)** SEM-EDS elemental maps of dolomite [$\text{CaMg}(\text{CO}_3)_2$] and its corresponding elements [Ca^{2+}] and [Mg^{2+}]. **(D)** and **(E)** SEM-EDS elemental maps of anhydrite [CaSO_4] and its corresponding elements [Ca^{2+}] and [S^{2-}]. Elemental data is depicted as higher readings of the specified element shown in white/pink and lower readings in darker green/blue. Anhydrite crystal size ranges from 10-30 μm and dolomite rhomboid size ranges from 10-20 μm .

SEM-BSE & SEM-EDS:

The SEM-BSE micrographs show three crystal types each with different atomic masses (note: higher atomic mass elements appear darker). SEM-EDS elemental maps (Figures 11B, 11C, 11D, and 11E) correlate strongly with the SEM-BSE micrographs (Figure 11A). High concentrations of calcium [Ca^{2+}] (Figure 11D) and sulfur [S^{2-}] (Figure 11E) (depicted as white and pink, respectively) correlate with the lightest shaded areas in the BSE images and are consistent with the presence of anhydrite [CaSO_4].

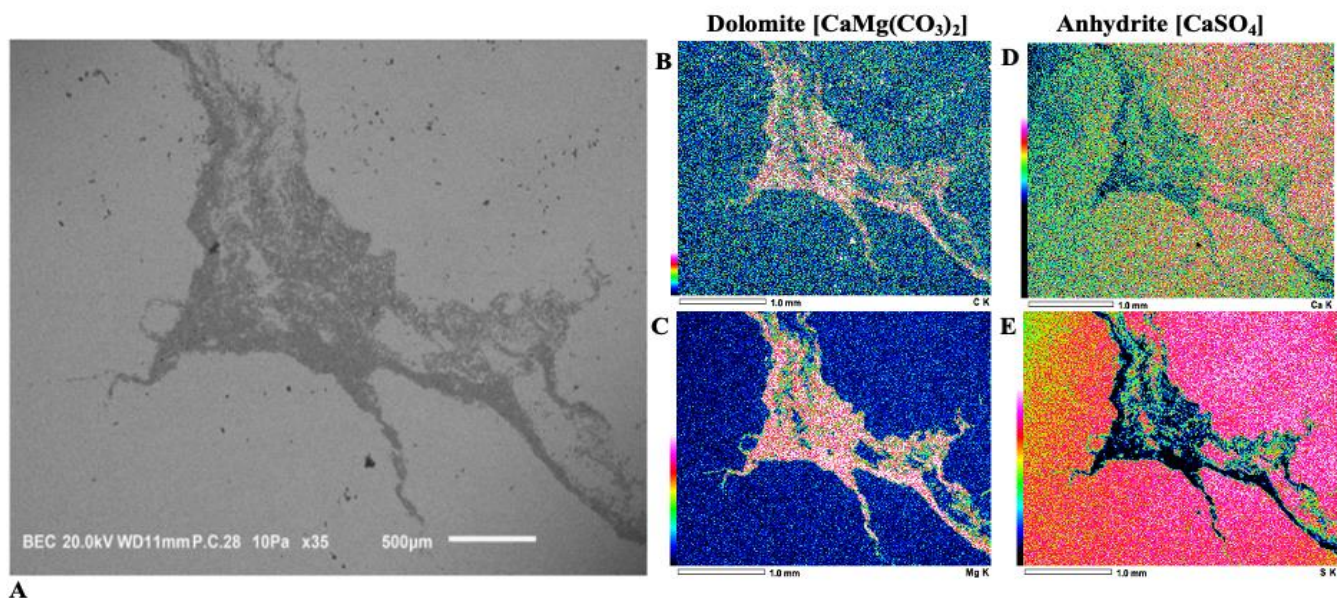


Figure 11. SEM-BSE and SEM-EDS photomicrographs of dolomite inclusion within nodular-anhydrite. **(A)** Thin section photomicrograph using backscatter at 35x shows compositional differences between dolomite inclusions within a blocky saccharoidal ground mass anhydrite supported by elements of dolomite $[\text{CaMg}(\text{CO}_3)_2]$. The contrast between different elements is presented as elements with a higher atomic mass appearing darker. **(B)** and **(C)** SEM-EDS elemental maps of dolomite $[\text{CaMg}(\text{CO}_3)_2]$ and its corresponding elements [C] and [Mg]. **(D)** and **(E)** SEM-EDS elemental map of anhydrite $[\text{CaSO}_4]$ and its corresponding elements [Ca] and [S]. Elemental data is depicted as higher readings of a specific element in white/pink and lower readings in darker green/blue.

Even though anhydrite $[\text{CaSO}_4]$ and dolomite both contain calcium $[\text{Ca}^{2+}]$, the EDS map for calcium (Figure 11D) shows higher counts (depicted as green and pink) for the large nodular masses mapped as anhydrite compared to the small rhombic crystals mapped as dolomite (depicted as blue). This is likely due to the different relative amounts of calcium $[\text{Ca}^{2+}]$ in anhydrite $[\text{CaSO}_4]$ and dolomite $[\text{CaMg}(\text{CO}_3)_2]$. The percent of subtotal mass for calcium $[\text{Ca}^{2+}]$ in anhydrite $[\text{CaSO}_4]$ is equal to 29.44%, whereas the percent of subtotal mass for calcium $[\text{Ca}^{2+}]$ in dolomite $[\text{CaMg}(\text{CO}_3)_2]$ is equal to 21.73%.

The elemental map for magnesium $[\text{Mg}^{2+}]$ (Figure 11C) shows higher concentrations (depicted as pink) within the second lightest BSE areas. The EDS data for carbon $[\text{C}^{4+}]$ (Figure 11B) also shows high values (depicted as pink) within the second lightest gray areas in the SEM-BSE micrograph. Collectively, the EDS elemental maps for magnesium, carbon, and calcium

suggest that the second lightest BSE contrast areas are dolomite [CaMg(CO₃)₂]. Note, this study did not attempt to determine the mineral with the heaviest atomic mass (appearing as the darkest grey in **Figure 11A**). The focus of this study was to determine the paragenesis between the dolomite and anhydrite of the Iutzi Member.

Conventional Isotope Analysis:

The measured dolomite $\delta^{18}\text{O}$ is -5.88 ‰ VPDB, and the $\delta^{13}\text{C}$ is 2.64‰ VPDB.

Table 4. Conventional stable isotope values from the dolomite subsample.

$\delta^{13}\text{C}$ (‰VPDB)	$\delta^{18}\text{O}$ (‰VPDB)
2.64	-5.88

Discussion:

Depositional Setting

The presence of evaporites and the lack of fauna in this section of core suggests evaporative conditions. Anhydrite with chicken wire texture (Figure 3) is generally interpreted as a displacive growth of gypsum in the vadose (unsaturated) zone of supratidal sabkha environments (Melvin, 1989). This texture reflects a restricted evaporative setting, where sediments are deposited and as anhydrite crystals grow, the deposited sediments and bedding become convoluted and destructed. These minerals and textures can be seen in modern restricted environments as well (James and Jones, 2015). For instance, the chicken wire habit of the anhydrite in Figure 3 is similar in habit to the nodular anhydrite that can be seen in the marginal marine sediments of the modern Persian Gulf. These Persian Gulf marginal sediments have played a major role in interpreting older evaporite deposits as paleosabkhas (Dean et al., 1975). Major anhydrite cyclothems in the Richfield Member have been reported in Melvin (1989), whereas each subsequent cycle of deposition was characterized by progressively more hypersaline water, creating an expansive and

thick package of evaporites. Although the facies of the “Massive Anhydrite” reflect an evaporative setting, the timing and geochemistry of the dolomite is more complicated to interpret.

Dolomite Petrography

The dolomite rhomboid $[\text{CaMg}(\text{CO}_3)_2]$ inclusions observed within the anhydrite $[\text{CaSO}_4]$ nodules in Figures 8, 9, and 10 suggests that the dolomite formed before the anhydrite. This observation is inconsistent the proposed evaporite driven dolomitization model that posits that as the evaporation of seawater occurs to a point where evaporite minerals, such as gypsum $[\text{CaSO}_4 \cdot 2\text{H}_2\text{O}]$ and anhydrite $[\text{CaSO}_4]$, form first and thus remove calcium $[\text{Ca}^{2+}]$ from the fluids, resulting in the Mg:Ca of the fluid to increase, thus driving the formation of dolomite $[\text{Ca}(\text{MgCO}_3)_2]$. If this model is the best way to explain the dolomites of the Iutzi Member, then it would be expected that the dolomites post-date the anhydrite.

Dolomite Stable Isotopes

The measured $\delta^{18}\text{O}$ value for the dolomite from the Iutzi Member is -5.88‰ VPDB (**Table 4**). This value is far more negative than what is expected for a mineral precipitated from evaporative fluids. Evaporative marine fluids are isotopically heavier than marine fluids (Rivers et al., 2019). This means, that dolomites formed via evaporative marine waters are expected to have greater $\delta^{18}\text{O}$ values than dolomite formed from marine fluids (Land, 1985).

The interpretation of the isotope data is not straightforward, however. The theoretical difference in fractionation between co-precipitating calcite and dolomite is reported to be $+3\text{‰}$ (Land 1985; Manche and Kaczmarek, 2019). The measured range of $\delta^{18}\text{O}$ VPDB values for marine calcites from the Lower Devonian fall between -5.5‰ VPDB to -2.5‰ VPDB (Henkes et al., 2018). Applying the theoretical $+3\text{‰}$ mineralogical fractionation between dolomite and

calcite, dolomites formed in Lower Devonian marine fluids would be expected to have $\delta^{18}\text{O}$ values that range between -2.5 ‰VPDB to +0.5 ‰VPDB. However, the $\delta^{18}\text{O}$ value for dolomite from the Iutzi Member is isotopically lighter by 3.38 ‰ compared to the lowest expected $\delta^{18}\text{O}$ value of dolomite derived from marine fluids from this time (Figure 12), which suggests that these dolomites did not form from evaporative fluids.

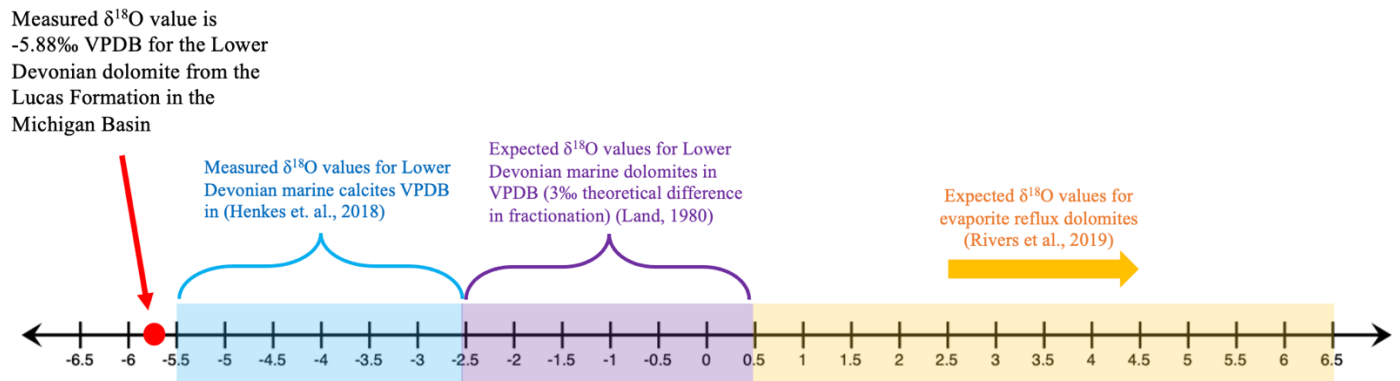


Figure 12. Dolomite conventional isotope data corrected for difference in fractionation (Land 1985) from the Lower Devonian age Lucas Formation of the Michigan Basin relative to the VPDB (Vienna Peedee belemnite) standard and compared to expected dolomite $\delta^{18}\text{O}$ ‰VPDB values for the lower Devonian formed from near-normal marine fluids (Henkes et al., 2018) and evaporative reflux fluids (Rivers et al., 2019).

There are two potential explanations for isotopically light dolomites in this study. One is that the dolomite was recrystallized at elevated temperatures during burial, and thus the isotopic signature was reset reflecting post-formation conditions (Ryan et al., 2020). A second explanation is that the dolomite originally formed from fluids that were isotopically lighter than Devonian seawater. Mixing between meteoric and marine fluids, for example, has been implicated in dolomitization (Badiozamani, 1973), though there has been much controversy on this topic (Machel, 2004). To explore these suggestions, more pXRD data should be taken to calculate the cation ordering of the dolomite as well as the clumped isotope data, which can be

used to determine the temperature of dolomite crystallization and the isotopic composition of the dolomitizing fluids (Ryan et al. 2023).

Conclusions:

The petrographical, mineralogical, and geochemical evidence reported here show that isotopically light microcrystalline dolomites formed before the pervasive anhydrite nodules that characterize the “Massive Anhydrite” unit of the Iutzi Member of the Lucas Formation. Collectively, these data are inconsistent with a model of dolomite formation by highly evaporated marine fluids, as is commonly posited for sedimentary dolomites co-occurring with evaporite minerals.

Acknowledgements

This thesis was completed under the help and instruction of Dr. Stephen Kaczmarek and Dr. Peter Voice. Much of the data sampled and collected for this thesis was conducted as part of an undergraduate class project at Western Michigan University for GEOS 5100: Advanced Earth Materials, under the help and supervision of Dr. Stephen Kaczmarek. Dr. Mohammed Al-Musawi provided guidance in sampling, analysis, and interpretation. Funding for this thesis was provided through the Western Michigan University College of Arts and Sciences Undergraduate Research and Creative Activities Grant. Discussions with Dr. Kaczmarek and the Carbonate Petrology and Characterization Lab team helped significantly improve this work through editing and revision.

References Cited:

- Adams, J., and Rhodes, M., 1960, Dolomitization by Seepage Refluxion, *Bulletin of the American Association of Petroleum Geologists*, Volume 44, pages 1912-1920.
- Al-Musawi, M., and Kaczmarek, S., 2020, A new carbonate-specific quantification procedure for determining elemental concentrations from portable energy-dispersive X-ray fluorescence (PXRF) data, *Applied Geochemistry*, Volume 113, 104491.
- Apak, S., 1985, Subsurface Stratigraphy and Sedimentologic Control on the Productive Middle Devonian Age Richfield Member of the Lucas Formation in the Michigan Basin, Master Thesis, Western Michigan University, Kalamazoo, MI.
- Badiozamani, K., The Dorag dolomitization model, application to the middle Ordovician of Wisconsin. *Journal of Sedimentary Research*, Volume 43, pages 965–984.
- Burns, M., Al-Musawi, M., and Kaczmarek, S.; 2023; Petrological Evidence of Early Dolomitization Followed by Nodular Gypsum-Anhydrite in the Lucas Formation, Michigan Basin, USA, GSA Sedimentary Geology Division, Geological Society of America *Abstracts with Programs*, Volume 55, page 3.
- Dean, W., Davies, G., and Anderson, R., 1975, Sedimentological Significance of Nodular and Laminated Anhydrite, *Geology*, Volume 3, pages 367-372.
- Downs, R., Bartelmehs, K., and Gibbs, G., 1993, Interactive Software for Calculating and Displaying X-Ray or Neutron Powder Diffractometer Patterns of Crystalline Materials, *The American Mineralogist*, Volume 78, pages 1104-1107.
- Gardner, W., 1974, Middle Devonian Stratigraphy and Depositional Environments in the Michigan Basin, Special Papers; *Michigan Basin Geological Society*, Volume 1, pages 36-37.

- Gregg, J., Bish, D., Kaczmarek, S., and Machel, H., 2015, Mineralogy, nucleation, and growth of dolomite in the laboratory and sedimentary environment: A review, *Sedimentology*, Volume 62, pages 1749–1769.
- Hardie, L., 1987, Dolomitization; a critical view of some current views, *Journal of Sedimentary Research*, Volume 57, pages 166–183.
- Henkes, G., Passey, B., Grossman, E., Shenton, B., Yancey, T., and Perez-Huerta, A., 2018, Temperature Evolution and the Oxygen Isotope Composition of Phanerozoic Oceans from Carbonate Clumped Isotope Thermometry, *Earth and Planetary Science Letters*, Volume 490, pages 40-50.
- Kaczmarek, S., and Thornton, B., 2017, The effect of Temperature on Stoichiometry, Cation Ordering, and Reaction Rate in High-Temperature Dolomitization Experiments, *Chemical Geology*, Volume 468, pages 32-41.
- Kaczmarek, S., and Sibley, D., 2007, A Comparison of Nanometer-scale Growth and Dissolution Features on Natural and Synthetic Dolomite Crystals; Implications for the Origin of Dolomite, *Journal of Sedimentary Research*, Volume 77, pages 424-432.
- Kaczmarek, S., and Sibley, D.; 2011, On the Evolution of Dolomite Stoichiometry and Cation Order During High-Temperature Synthesis Experiments: An Alternative Model for the Geochemical Evolution of Natural Dolomites, *Sedimentary Geology*, Volume 240, pages 30-40.
- Kaczmarek, S., and Sibley, D., 2014, Direct physical evidence of dolomite recrystallization, *Sedimentology*, Volume 61, no. 6, pages 1862-1882.

- Kaczmarek, S., Gregg, J., Bish, D., Machel, H., and Fouke, B.; 2017, Dolomite, very high-magnesium calcite, and microbes—implications for the microbial model of dolomitization, *SEPM (Society for Sedimentary Geology)*, Volume 109, pages 7-20.
- James, N., and Jones, B.; 2016, Origin of Carbonate Sedimentary Rocks, *Wiley: American Geophysical Union*.
- Land, L., 1985, The Origin of Massive Dolomite, *Journal of Geological Education*, Volume 33, pages 112-125.
- Laya, J., Teoh, C., Whitaker, F., Manche, C., Kaczmarek, S., Tucker, M., Gabellone, T., and Hasiuk, F.; 2021, Dolomitization of a Miocene-Pliocene progradational carbonate platform by mesohaline brines: Re-examination of the reflux model on Bonaire Island, *Marine and Petroleum Geology*, 126, 104895.
- Lilienthal, R., 1978, Stratigraphic Cross-Sections of the Michigan Basin, Department of Natural Resources, State of Michigan, *Geological Survey Division*, pages 13-15.
- Lumsden, D., and Chimahusky, J., 1980, Relationship between Dolomite Nonstoichiometry and Carbonate Facies Parameters, *The Society of Economic Paleontologists and Mineralogists (SEPM)*, Volume 28, pages 123-137.
- Machel, H., 2004, Concepts and models of dolomitization: a critical reappraisal, *The Geometry and Petrogenesis of Dolomite Hydrocarbon Reservoirs*, Volume 235, pages 7–63.
- Manche, C., and Kaczmarek, S.; 2019; Evaluating reflux dolomitization using a novel high-resolution record of dolomite stoichiometry: A case study from the Cretaceous of central Texas, USA; *The Geological Society of America*, Volume 47, pages 586-590.

- Manche, C., and Kaczmarek, S., 2021, A Global Study of Dolomite Stoichiometry and Cation Ordering through the Phanerozoic, *Journal of Sedimentary Research*, Volume 95, pages 520-546.
- Park, S., 1987, Deposition, Diagenesis and Porosity Development of the Middle Devonian, Lucas Formation in the West Branch Oil Field, Ogemaw County, Michigan: Master Thesis, Western Michigan University, Kalamazoo, MI.
- Rivers, J., Varghese, L., Yousif, R., Whitaker, F., Skeat, S., and Al-Shaikh, I., 2019. The Geochemistry of Qatar Coastal Waters and its Impact on Carbonate Sediment Chemistry and Early Marine Diagenesis, *Journal of Sedimentary Research*, Volume 89, pages 293-303.
- Ryan, B., Kaczmarek, S., and Rivers, J.; 2020; Early and pervasive dolomitization by near-normal marine fluids: New lessons from an Eocene evaporative setting in Qatar; *Journal of the International Association of Sedimentologists*; Volume 67, pages 2917-2944.
- Ryan, B., Rivers, J., Petersen, S., and Kaczmarek, S.; 2023, Evidence of nonplanar dolomite textures formed at near-surface temperatures, *Journal of Sedimentary Research*, Volume 93, pages 729-740.